


Synthesis, spectroscopic characterization, and antimicrobial activities of Ni(II) and Fe(II) complexes with *N*-(2-hydroxyethyl)-5-nitrosalicylaldimine

Selma Celen, Elif Gungor, Hulya Kara & A. Dilek Azaz


To cite this article: Selma Celen, Elif Gungor, Hulya Kara & A. Dilek Azaz (2013) Synthesis, spectroscopic characterization, and antimicrobial activities of Ni(II) and Fe(II) complexes with *N*-(2-hydroxyethyl)-5-nitrosalicylaldimine, Journal of Coordination Chemistry, 66:18, 3170-3181, DOI: 10.1080/00958972.2013.829568

To link to this article: <https://doi.org/10.1080/00958972.2013.829568>

 View supplementary material 

 Accepted author version posted online: 26 Jul 2013.
Published online: 02 Sep 2013.

 Submit your article to this journal 

 Article views: 155

 View related articles 

 Citing articles: 18 View citing articles 

Synthesis, spectroscopic characterization, and antimicrobial activities of Ni(II) and Fe(II) complexes with *N*-(2-hydroxyethyl)-5-nitrosalicylaldimine

SELMA CELEN[†], ELIF GUNGOR^{*‡}, HULYA KARA[‡] and A. DILEK AZAZ[†]

[†]Faculty of Science and Art, Department of Biology, Balikesir University, Balikesir, Turkey

[‡]Faculty of Science and Art, Department of Physics, Balikesir University, Balikesir, Turkey

(Received 21 March 2013; accepted 2 July 2013)

Metal complexes [Ni(HL1)₂H₂O] (**1**) and [Fe(HL1)₂] (**2**), where **HL1** is the tridentate Schiff base *N*-(2-hydroxyethyl)-5-nitrosalicylalimine, were synthesized and characterized by spectroscopic methods. The crystal structures of **1** and **2** have been determined by single crystal diffraction at 100 K. Complexes **1** and **2** have a distorted octahedral geometry. The ligand and metal complexes were screened for antibacterial and antifungal activities by the disk diffusion, microdilution broth, and single spore culture techniques. Antimicrobial activities of the ligand and its complexes have been tested against 10 bacteria, two yeast, and five filamentous fungi. The ligand and metal complexes were found to be active against all tested micro-organisms.

Keywords: Schiff base; Nickel(II); Iron(II); Antibacterial activity; Antifungal activity

1. Introduction

Schiff bases and their transition metal compounds have numerous biological and medicinal applications. Schiff base compounds have been used in medicine as antibiotic, antiallergic, antitumoral [1], antibacterial, and antifungal agents [2–12]. Metal ions present in complexes accelerate the drug action and the efficacy of the organic therapeutic agents [13, 14]. Development of new and effective antibacterial and antifungal drugs has become an urgent task for infectious diseases [15, 16]. The biological activities of the newly prepared compounds may be more effective than well-known classes of antimicrobial agents to which many clinically relevant pathogens are resistant. To establish structure-biological activity relationships, numerous transition metal complexes have been studied [17–19]. They exhibit strong or weak biological activity associated with different coordinations of Schiff bases with metal ions such as copper, cobalt, nickel, iron, and manganese [2–22]. In the present work, this field is extended by synthesis of mononuclear Ni(II) and Fe(II) Schiff base complexes.

Although there has been considerable interest in characterization, antibacterial and antifungal properties of salen-type Schiff base metal complexes [2–22], little attention has been

*Corresponding author. Email: egungor@balikesir.edu.tr

paid to systems that contain Fe(II) [17–19]. For this reason here we report the preparation, characterization, antibacterial and antifungal properties of **HL1** and its Ni(II) and Fe(II) complexes, $[\text{Ni}(\text{HL1})_2\text{H}_2\text{O}]$ (**1**) and $[\text{Fe}(\text{HL1})_2]$ (**2**), against 10 bacteria, two yeast and five filamentous fungi.

2. Experimental

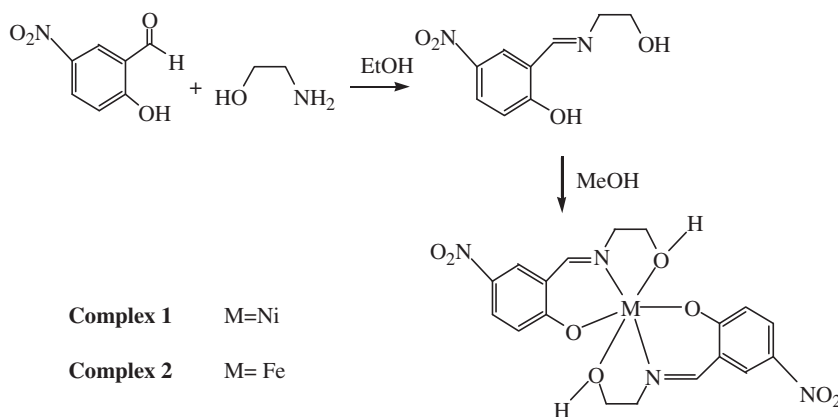
2.1. Materials and physical measurements

All chemical reagents and solvents were purchased from Merck or Aldrich and used without purification. Elemental (C, H, N) analyzes were carried out by standard methods with a LECO, CHNS-932 analyzer. UV–vis spectra were carried out at 20 °C on a Perkin–Elmer Lambda 25 UV–Vis spectrometer. FT-IR spectra were measured with a Perkin–Elmer Model Bx 1600 instrument with samples as KBr pellets from 4000 to 400 cm^{-1} . ^1H and ^{13}C NMR spectra of **HL1** were recorded in DMSO on a Bruker Biospin (300 MHz). The melting points of the ligand and complexes were determined on a Buchi M-560 melting point apparatus. The synthetic route of **HL1**, **1** and **2** are outlined in scheme 1.

2.2. Synthesis of HL1

The tridentate Schiff base **HL1** was prepared by mixing 2-hydroxy-5-nitrobenzaldehyde (1 mM) and ethanolamine (1 mM) in 1:1 M ratio in hot ethanol (50 cm^3). The solution obtained was stirred at 78 °C for 30 min. The yellow compound precipitated from the solution on cooling.

HL1: Yellow crystals, yield 82%. Melting point: 114.8–116.6 °C. Calcd: C, 51.43; H, 4.80; N, 13.33. Experimentally found composition (in %): C, 51.39; H, 4.82; N, 13.31%. ^1H NMR (DMSO, δ ppm) yielded signals at: 3.83–3.93 (– $\text{NCH}_2\text{CH}_2\text{OH}$, 4H), 5.15 (– $\text{NCH}_2\text{CH}_2\text{OH}$, 1H), 6.59 (– $\text{CH}=\text{CHOH}$ –, 1H), 8 (– $\text{CHNO}_2=\text{CH}$ –), 8.4 (– $\text{CH}(\text{NO}_2)-\text{CH}=\text{CH}$ –, 1H), 8.6 (– $\text{CH}=\text{N}$ –, 1H). ^{13}C NMR (DMSO, δ ppm) yielded signals at: 54.85 (– $\text{N}-\text{CH}_2$ –), 59.73 (– HOCH_2 –), 113.79 (– $\text{CH}=\text{CHOH}$ –), 123.40 (– $\text{CH}=\text{CH}-\text{COH}$ –), 139.79 (– $\text{CH}=\text{CH}-\text{COH}$ –), 133.30 (– $\text{CH}=\text{CNO}_2$ –), 133.89 (– $\text{CH}=\text{CNO}_2$ –), 168.22 (– $\text{C}=\text{COH}$ –), 178.74 (– $\text{C}=\text{N}$ –).



Scheme 1. The synthetic route of **HL1**, **1** and **2**.

The IR (KBr) spectrum showed signals (in cm^{-1}) at: 3134, 3102, 3098, 3047, 2838, 2742, 1658, 1602, 1319, 1292, 1244, 1175. The UV–Vis (DMF) spectrum had peaks (in nm) at: 335, 417.

2.3. Synthesis of **1** and **2**

Complex **1** was prepared by the addition of nickel(II) acetate tetrahydrate (0.248 g, 1 mM) in 40 cm^3 of hot methanol to **HL1** (1 mM) in 30 cm^3 of hot ethanol. This solution was warmed to 78°C and stirred for 30 min. A green solution was obtained and allowed to stand at room temperature. Several weeks of standing led to the growth of green crystals. Complex **2** was prepared in a similar way using iron(II) chloride tetrahydrate (0.198 g, 1 mM) instead of nickel(II) acetate tetrahydrate in hot methanol.

In general, iron can form stable compounds in both the divalent and trivalent states depending on the conditions. Iron(II) complexes with Schiff bases are air sensitive and easily oxidized to iron(III) complexes by molecular oxygen. In the presence of oxygen, iron(II) complexes are stable only under acidic conditions ($\text{pH} < 4$); at neutral pH ($\text{pH} > 4$) they are rapidly oxidized to iron(III) [23, 24]. The synthesis was performed under aerobic conditions with an acidic pH of 3.2 for complex **2**.

Complex **1**: Green crystals yield 75%. Melting point: $172.4\text{--}183.4^\circ\text{C}$. Theoretical composition (in %): C, 43.67; H, 4.07; N, 11.32. Experimentally found composition (in %): C, 43.64; H, 4.09; N, 11.34%. The IR (KBr) spectrum showed signals (in cm^{-1}) at: 3201, 2910, 2784, 1652, 1439, 1395, 1378, 647, 588, 550, 536, 513, 474, 450, 429. UV–Vis (DMF) nm: 256, 395, 602.

Complex **2**: Dark-red crystals yield 75%. Melting point: $109.8\text{--}110.7^\circ\text{C}$. Theoretical composition (in %): C, 45.59; H, 3.83; N, 11.81. Experimentally found composition (in %): C, 45.61; H, 3.80; N, 11.83%. The IR (KBr) spectrum showed signals (in cm^{-1}) at: 3067, 2918, 2728, 1616, 1451, 1395, 1342, 651, 562, 544, 493, 474, 435, 413. The UV–Vis (DMF) spectrum had peaks (in nm) at: 271, 407, 657.

2.4. X-ray structure determination

Diffraction measurements were made on a Bruker ApexII Kappa CCD diffractometer using graphite-monochromated Mo-K_α radiation ($\lambda = 0.71073 \text{ \AA}$) at 100 K. The intensity data were integrated using APEXII [25]. Absorption corrections were applied based on equivalent reflections using SADABS [26]. The structures were solved by direct methods and refined using full-matrix least-squares against F^2 with SHELXL [27]. All non-hydrogen atoms were assigned anisotropic displacement parameters and refined without positional constraints. Hydrogens were included in idealized positions with isotropic displacement parameters constrained to 1.5 times the U_{equiv} of their attached carbon for methyl hydrogens and 1.2 times the U_{equiv} of their attached carbon for all others. Hydrogens of water were located in a difference Fourier map and refined isotropically. Distance restraints were also applied to hydrogens of water with a set value of $0.90(1) \text{ \AA}$. The absolute structure of **1** was determined on the basis of the Flack [28] parameter $x = 0.004(11)$. Flack parameter close to 0 is indicative of a non-centrosymmetric structure. Methanol in the crystal lattice of **2** appears to be highly disordered, and it was difficult to model reliable positions. Therefore, the SQUEEZE function of PLATON [29] was used to eliminate the contribution of the electron density in the solvent region from the intensity data, and the solvent-free model was employed for the final refinement.

2.5. Biological activity

HL1, 1, and 2 were subjected to screening for antimicrobial activity by using agar disk diffusion assay, microdilution broth assay [30, 31], and single spore culture technique (for filamentous fungi) [32]. The antimicrobial activities of **L1, 1, and 2** were evaluated against 10 bacteria *Campylobacter jejuni* (ATCC 3291), *Enterobacter aerogenes* (NRRL 3567), *Escherichia coli* (ATCC 25292), *Listeria monocytogenes* (ATCC 7644), *Pseudomonas aeruginosa* (ATCC 27853), *Proteus vulgaris* (NRRL 123), *Staphylococcus aureus* (ATCC 6538), *Serratia marcescens* (clinical isolate), *Shigella sonnei* (ATCC 25931), and *Klebsiella pneumoniae* (clinical isolate), two yeasts *Candida albicans* (ATCC 10231) and *C. albicans* (clinical isolate) and five filamentous fungi *Aspergillus flavus*, *Aspergillus niger*, *Penicillium expansum*, *Penicillium lanosum*, and *Alternaria alternata*. (The tested microfungi were isolated from soil in our department.)

2.5.1. Agar disk diffusion method. The agar disk diffusion method was employed for determination of antimicrobial capacities of **L1, 1, and 2** [30]. A suspension of the tested micro-organism (500 μL of 10^8 CFU/mL) was spread on the solid media plates. Each test solution was prepared in DMF. Then filter paper disks (6 mm in diameter) were soaked in 20 μL of the stock solutions and placed on inoculated plates. After keeping at 2 $^\circ\text{C}$ for 2 h, they were incubated at 37 $^\circ\text{C}$ for 24 h for bacteria and *C. albicans* (*C. jejuni* was incubated at 42 $^\circ\text{C}$, microaerophilic conditions for 48 h). The diameters of the inhibition zones were measured in millimeters. Each test was carried out in triplicate and the average was calculated for inhibition zone diameters.

2.5.2. The microdilution broth method. A microdilution broth susceptibility assay was used for the determination of minimum Inhibitory concentration (MIC) [31]. Serial dilutions of compounds were prepared in sterile distilled water in 96-well microtitre plates. Freshly grown bacterial suspension was standardized to 10^8 CFU/mL (McFarland No. 0.5) in double strength Mueller-Hinton Broth (*L. monocytogenes* in Buffered Listeria Enrichment Broth and yeast suspension of *C. albicans* in Saboraud Dextrose Broth). Sterile distilled water served as growth control. Hundred microlitre of each microbial suspension was then added to each well. The last row containing only the serial dilutions of antibacterial agent without micro-organism was used as negative control. After incubation at 37 $^\circ\text{C}$ for 24 h (*C. jejuni* was incubated at 42 $^\circ\text{C}$ microaerophilic conditions for 48 h) the first well without turbidity was determined as the MIC. Chloramphenicol (1000 $\mu\text{g}/\text{mL}$) and ketoconazole (1000 $\mu\text{g}/\text{mL}$) served as positive controls. Each test was performed in triplicate.

2.5.3. Antifungal studies. In order to obtain conidia, the fungi were cultured on Czapek Dox Agar and Malt Extract Agar medium (Merck) in 9 cm Petri dishes at 25 $^\circ\text{C}$ for 7–10 days. Harvesting was carried out by suspending the conidia in 1% (w/v) sodium chloride solution containing 5% (w/v) DMSO. The spore suspension was then filtered, transferred into tubes and, stored at -20 $^\circ\text{C}$, accordingly to Hadecek and Greger [33]. The 1 mL spore suspension was taken and diluted in a loop drop until one spore could be captured. One loop drop from the spore suspension was applied onto the center of the Petri dish containing Czapek Dox Agar and Malt Extract Agar. 20 μL of each complex was applied onto sterile paper disks (6 mm in diameter) and placed in the petri dishes and

incubated at 25 °C for 72 h. Spore germination during the incubation period was followed using a microscope (Olympus BX51) in 8 h intervals. The inhibition of fungal growth expressed in percentage was determined on the growth in test plates compared to the respective control plates [34].

$$\text{Inhibition \%} = 100 \times \frac{C - T}{C}$$

where C is the diameter of fungal growth on the control, T is the diameter of fungal growth on the test plate.

The activities of the complexes have been compared with the activity of standard antifungicide ketoconazole.

3. Results and discussion

3.1. X-ray structure determinations of **1** and **2**

Crystallographic data conditions used for intensity data collection and some features of the structure refinement are listed in table 1. Perspective ORTEP views with atom-labeling scheme of **1** and **2** are presented in figures 1 and 2, respectively. Selected bond lengths and angles are given in table 2.

Complexes **1** and **2** crystallize in the orthorhombic space group $P2_12_12_1$ and $Fddd$, respectively. The asymmetric unit of **1** consists of one chiral monomeric $[\text{Ni}(\text{HL}1)_2]$ unit with water, while **2** consists of half of the monomeric $[\text{Fe}(\text{HL}1)]$ unit with methanol. N -(2-hydroxyethyl)-5-nitrosalicylalimine is monoanionic, tridentate with ONO donor set coordinating through one imine nitrogen (N_{imi}), one alkoxy oxygen (O_{alk}), and a deprotonated phenol (O_{phe}). The six-coordinate nickel and iron are defined by two imine nitrogens,

Table 1. Crystal data and structure refinement for **1** and **2**.

	1	2
Empirical formula	$\text{C}_{18}\text{H}_{20}\text{N}_4\text{NiO}_9$	$\text{C}_{18}\text{H}_{18}\text{N}_4\text{FeO}_8$
Formula weight (g mol^{-1})	495.09	474.21
Temperature (K)	100(2)	100(2)
Crystal system	Orthorhombic	Orthorhombic
Space group	$P2_12_12_1$	$Fddd$
Unit cell dimensions	$a = 9.5566(11) \text{ \AA}$, $\alpha = 90^\circ$ $b = 12.8963(16) \text{ \AA}$, $\beta = 90^\circ$ $c = 16.047(2) \text{ \AA}$, $\gamma = 90^\circ$	$a = 10.2723(3) \text{ \AA}$, $\alpha = 90^\circ$ $b = 23.7900(9) \text{ \AA}$, $\beta = 90^\circ$ $c = 36.5054(12) \text{ \AA}$, $\gamma = 90^\circ$
Volume (\AA^3)	1977.7(4)	8921.1(5)
Z	4	16
Density (calculated) (g cm^{-3})	1.663	1.412
Absorption coefficient (mm^{-1})	1.044	0.726
θ range for data collection ($^\circ$)	2.0–27.5	2.0–27.6
Index ranges	$-12 \leq h \leq 9$, $-13 \leq k \leq 16$, $-20 \leq l \leq 14$	$-13 \leq h \leq 13$, $-30 \leq k \leq 30$, $-47 \leq l \leq 47$
Reflections collected	10,147	37,296
Independent reflections	4448	2591
Data/restraints/parameters	3762/4/301	2408/1/145
Goodness-of-fit on F^2	1.02	1.18
R indices [$I > 2\sigma(I)$]	$R_1 = 0.0305$, $wR_2 = 0.0668$	$R_1 = 0.0370$, $wR_2 = 0.0881$
Largest diff. peak and hole ($\text{e}\text{\AA}^{-3}$)	0.44 and -0.47	0.35 and -0.51
Flack parameter	0.004 (11)	–

two phenoxo oxygens, and alcoholic oxygens. The average bond lengths are Ni–O_{phe} = 2.02 (17) Å, Ni–O_{alk} = 2.12(17) Å, and Ni–N_{imi} = 2.00(2) Å for **1**, and Fe–O_{phe} = 1.94(15) Å, Fe–O_{alk} = 2.01(13) Å, and Fe–N_{imi} = 2.12(15) Å for **2**, respectively. The angles around the metal in the six-membered chelate ring are slightly distorted. Therefore, **1** and **2** have a distorted octahedral geometry being chelated by two tridentate Schiff base ligands. The angles O–M–O (M=Ni, Fe) are 87.81(7)–91.59(7)° for **1** and 90.34(5)–91.41(6)° for **2** and the angles dealing with O–M–N are 81.44(8)–96.11(8)° for **1** and 86.07(6)–90.37(6)° for **2**; the N–M–N angle is 175.51(8)° for **1** and 165.39(7)° for **2**. Selected bond lengths and angles, listed in table 1, lie within the range of reported values for corresponding bond lengths and angles of other mononuclear nickel(II) [35, 36] and iron(II) complexes [37, 38].

In **1** and **2**, adjacent molecules are linked through intermolecular O–H···O hydrogen bonds (table 3, figures 3 and 4). Molecules interacting through O–H···O hydrogen bonds in **1** give a 3-D coordination network. The structure of **1** is observed in the *bc*-plane, stacked orthogonally to the *a*-axis. Intermolecular hydrogen bonding of **2** assembles the molecular units leading to ordered zigzag chain structures. This intermolecular interaction results in the formation of 1-D networks. The zigzag chain structures propagate along the crystallographic *a* axis.

3.2. FTIR spectroscopy

The IR spectra of **1** and **2** were analyzed in comparison with that of their free ligand **HL1** from 4000–400 cm⁻¹. The strong sharp absorption at 1661 cm⁻¹ in spectra of **HL1** can be assigned to C=N stretch; in the complexes, these bands are shifted to lower frequencies attributed to the coordination of the imine nitrogen. Bands at 1652 and 1597 cm⁻¹ are assigned to the imine stretch in **1** and **2**, respectively [39]. IR spectra of **HL1** show a broad band at 3134–3047 cm⁻¹ due to O–H stretch, which disappears in the respective complexes indicating deprotonation of the Schiff base upon complexation. Several weak peaks observed for the complexes at 3201–2728 cm⁻¹ are due to aromatic and aliphatic C–H stretches. The C–N stretches for **1** and **2** are in the range 1451–1342 cm⁻¹. Aromatic nitro compounds of **HL1** and complexes have absorptions due to asymmetric and symmetric stretches of C–NO₂ at 1597–1549 and 1395–1378 cm⁻¹, respectively. Ligand coordination

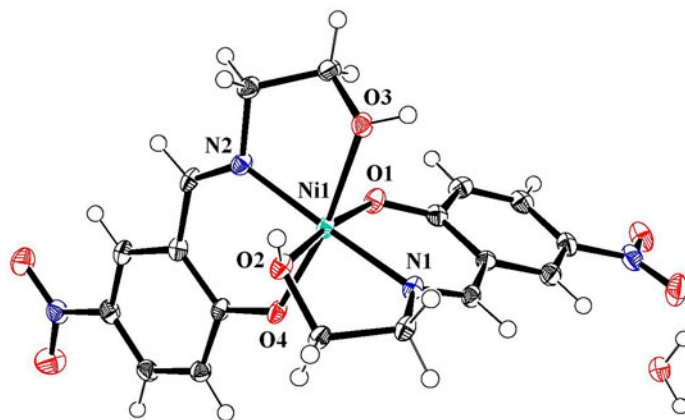
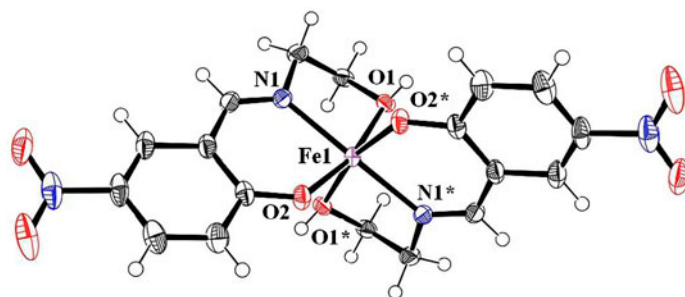


Figure 1. ORTEP drawing of **1** with atom labeling. Thermal ellipsoids have been drawn at 50% probability level.

Figure 2. ORTEP drawing of **2** with atom labeling. Thermal ellipsoids have been drawn at 50% probability level.Table 2. Selected bond lengths [Å] and angles [°] for **1** and **2**.

1		2	
<i>Bond lengths</i>			
Ni1–O1	2.01(16)	Fe1–O1	2.01(13)
Ni1–O2	2.09(16)	Fe1–O2	1.94(15)
Ni1–O3	2.15(19)	Fe1–O1*	2.01(13)
Ni1–O4	2.03(18)	Fe1–O2*	1.94(15)
Ni1–N1	2.01(2)	Fe1–N1	2.12(15)
Ni1–N2	2.00(2)	Fe1–N1*	2.12(15)
<i>Bond angles</i>			
O1–Ni1–O3	90.31(7)	O1–Fe1–O1*	90.34(5)
O1–Ni1–O4	91.42(7)	O1–Fe1–O2*	91.41(6)
O2–Ni1–O3	91.59(7)	O2–Fe1–O1*	91.41(6)
O2–Ni1–O4	87.81(7)	O2–Fe1–O2*	90.61(6)
O1–Ni1–N1	91.51(8)	O1–Fe1–N1	79.30(6)
O1–Ni1–N2	91.17(8)	O1–Fe1–N1*	90.37(6)
O2–Ni1–N1	81.44(8)	O2–Fe1–N1	86.07(6)
O2–Ni1–N2	95.95(8)	O2–Fe1–N1*	104.32(6)
O3–Ni1–N1	96.11(8)	O1*–Fe1–N1	90.37(6)
O3–Ni1–N2	80.27(8)	O2*–Fe1–N1	104.32(6)
O4–Ni1–N1	93.01(8)	O1*–Fe1–N1*	79.30(6)
O4–Ni1–N2	90.53(8)	O2*–Fe1–N1*	86.07(6)
N1–Ni1–N2	175.51(8)	N1–Fe1–N1*	165.39(7)

Note: The asymmetric unit of **2** consists of half of the monomeric [Fe(HL1)] unit. The other half of the molecule is symmetric. Therefore, symmetrical atoms in the molecule are shown with * symbol.

Table 3. Hydrogen bond geometry (Å, °) of **1** and **2**.

	D–H···A	D–H	H···A	D···A	D–H···A
1	O7–H7A···O9 ⁽ⁱ⁾	0.8800	2.02	2.866	162.00
	O7–H7A···O1 ⁽ⁱⁱ⁾	0.8600	2.33	3.113	150.00
	O2–H19···O4 ⁽ⁱⁱⁱ⁾	0.8800	1.83	2.683	162.00
	O3–H20···O7 ^(iv)	0.8400	1.87	2.700	167.00
2	O1–H1A···O1 ^(v)	0.8100	1.72	2.464	153.00

Notes: Symmetry codes: ⁽ⁱ⁾1 + x, 1 + y, z; ⁽ⁱⁱ⁾1 – x, –1/2 + y, 3/2 – z; ⁽ⁱⁱⁱ⁾–1/2 + x, 1/2 – y, 2 – z; ^(iv)–1 + x, y, z; ^(v)3/4 – x, 3/4 – y, z. The asymmetric unit of **2** consists of half of the monomeric [Fe(HL1)] unit. The other half of the molecule is symmetric. Therefore, symmetrical atoms in the molecule are shown with * symbol.

to the metal center is substantiated by bands at 647–474 and 450–413 cm^{–1}, attributable to $\nu(\text{M–N})$ and $\nu(\text{M–O})$, respectively, observed in all the complexes.

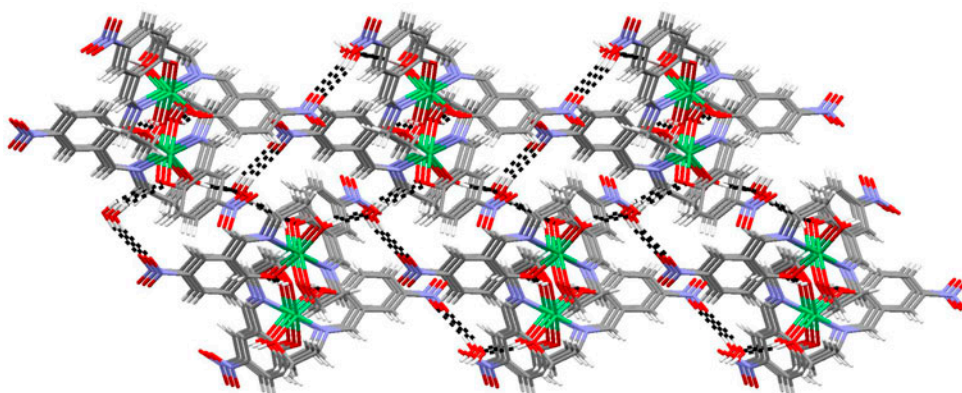


Figure 3. A 3-D network structure formed by hydrogen bonds in the *bc*-plane of **1**. Dotted lines indicate hydrogen bonds.

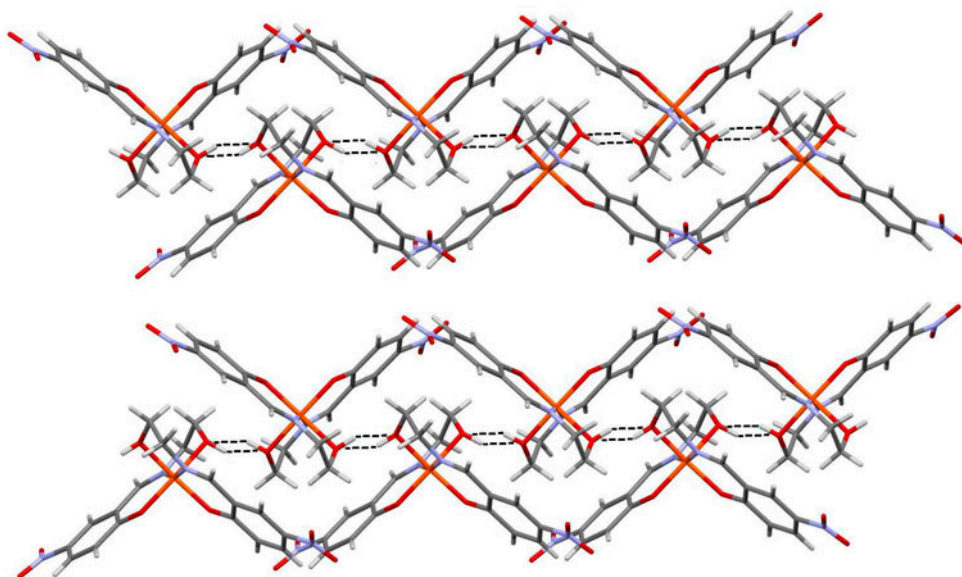


Figure 4. A 1-D network structure formed by hydrogen bonds of **2**. Dotted lines indicate hydrogen bonds.

3.3. Electronic spectra

UV–Visible spectra of **HL1**, **1**, and **2** were carried out in DMF. The electronic transitions due to the ligand in **1** and **2** showed the absorptions of the $\pi \rightarrow \pi^*$ and $n \rightarrow \pi^*$ transitions of C=N at 253–407 nm regions. These values are lower than the corresponding absorption for **HL1**, at 335 and 417 nm, respectively. This may be due to the coordination of nitrogen and oxygen. The UV–Vis spectrum of **1** exhibits two absorptions at 256 and 395 nm, while these are at 253 and 407 nm for **2** (figures S1 and S2). It was not possible to identify d–d

transitions due to a strong charge transfer band tailing from UV to the visible region [40, 41].

3.4. Antibacterial and antifungal activities

The antimicrobial activities of ligand and complexes have been tested *in vitro* by agar disk diffusion (table 4), microdilution broth susceptibility assay (table 5), and single spore culture technique (table 6) against micro-organisms which are known to cause food spoilage and infections in humans. The activity data show that the complexes are more potent antimicrobial agents than the free ligand. Chloramphenicol (1000 µg/mL) and ketoconazole (1000 µg/mL) served as positive controls. Chloramphenicol and ketoconazole showed strong antimicrobial activity against all the micro-organisms tested.

The results of agar disk diffusion assay (table 4) exhibit that Ni(II) and Fe(II) complexes and the free ligand affect bacteria and yeasts because they show clear inhibition zones with the tested bacteria and yeast on solid agar media. At the end of incubation, the diameters of the inhibition zones are in the range 7–10 mm. If the inhibition zone measures 2–3 mm, then the complex has good antimicrobial activity. If the inhibition zone is more than 3 mm across, then it is considered very effective, but if there is no inhibition zone then the complex has no activity on the bacterium [42]. Ni(II) and Fe(II) complexes have high antimicrobial activity against *P. aeruginosa*, *E. coli*, and *S. aureus* with inhibitions zones of 10 mm.

The Ni(II) and Fe(II) complexes exhibited similar levels of antimicrobial activity. Fe(II) is most effective against *P. vulgaris* and *S. marcescens* with an MIC value of 125 µg/mL. Ni(II) and Fe(II) complexes have higher antibacterial activity than the free ligand. This enhancement in activity may be due to an efficient diffusion of the metal complexes into the bacterial cell and/or interaction with the bacterial cell [43]. Previously we studied the antibacterial and antifungal activities of Co(III) complexes [Co(HL1)(L1)](1) and [Co(HL2)(L2)](2) [where HL1 = 2-((E)-(2-hydroxyethylimino)methyl)-4-chlorophenol and HL2 = 2-((E)-(2-hydroxyethylimino)methyl)-4-bromophenol] using agar disk diffusion and microdilution broth susceptibility assay. The results obtained showed that Co(III) complexes demonstrated antimicrobial activity against all tested micro-organisms [22] as well as Ni(II) and Fe(II) complexes showed higher antibacterial activities than Co(III) complexes. The variation in the

Table 4. Inhibition zones of the ligand and complexes according to agar disc diffusion method [mm].

Microorganisms	Sources	1	L1	2	Standard
<i>Campylobacter jejuni</i>	ATCC 33291	9	8	9	10 ^C
<i>Enterobacter aerogenes</i>	NRRL 3567	9	8	9	9 ^C
<i>Escherichia coli</i>	ATCC 25292	10	9	10	11 ^C
<i>Listeria monocytogenes</i>	ATCC 7644	9	7	9	10 ^C
<i>Pseudomonas aeruginosa</i>	ATCC 27853	10	9	10	10 ^C
<i>Proteus vulgaris</i>	NRRL 123	9	8	9	10 ^C
<i>Staphylococcus aureus</i>	ATCC 6538	10	9	10	10 ^C
<i>Serratia marcescens</i>	Clinical isolate	9	8	9	9 ^C
<i>Shigella sonnei</i>	ATCC 25931	9	8	9	9 ^C
<i>Klebsiella pneumoniae</i>	Clinical isolate	9	8	9	9 ^C
<i>Candida albicans</i>	ATCC 10231	8	8	9	9 ^K
<i>Candida albicans</i>	Clinical isolate	9	8	9	9 ^K

Notes: ^CChloramphenicol (1000 µg/mL).

^KKetoconazole (1000 µg/mL).

Table 5. MIC [$\mu\text{g/mL}$] of the ligand and complexes.

Microorganisms	Sources	1	L1	2	Standard
<i>Campylobacter jejuni</i>	ATCC 33291	125	250	125	250 ^C
<i>Enterobacter aerogenes</i>	NRRL 3567	125	250	125	250 ^C
<i>Escherichia coli</i>	ATCC 25292	125	250	125	125 ^C
<i>Listeria monocytogenes</i>	ATCC 7644	125	250	125	125 ^C
<i>Pseudomonas aeruginosa</i>	ATCC 27853	125	125	125	250 ^C
<i>Proteus vulgaris</i>	NRRL 123	250	250	125	125 ^C
<i>Staphylococcus aureus</i>	ATCC 6538	125	250	125	125 ^C
<i>Serratia marcescens</i>	Clinical isolate	250	250	125	250 ^C
<i>Shigella sonnei</i>	ATCC 25931	125	250	125	250 ^C
<i>Klebsiella pneumoniae</i>	Clinical isolate	125	250	125	250 ^C
<i>Candida albicans</i>	ATCC 10231	250	250	250	250 ^K
<i>Candida albicans</i>	Clinical isolate	125	250	125	250 ^K

Notes: ^CChloramphenicol (1000 $\mu\text{g/mL}$).

^KKetoconazole (1000 $\mu\text{g/mL}$).

Table 6. Antifungal activities for the tested complexes (inhibition %).

Filamentous fungi	1	HL1	2	Ketoconazole
<i>Aspergillus flavus</i>	20	12.5	25	83.63
<i>Aspergillus niger</i>	35.1	21.6	29.7	40
<i>Penicillium expansum</i>	33.3	19	23.8	65
<i>Penicillium lanosum</i>	28.5	9.5	28.5	54
<i>Alternaria alternata</i>	22.2	20.4	22.8	82

activity of the metal complexes against different organisms depends on the impermeability of the micro-organisms' cells or on differences in the ribosome of the microbial cells [44].

The antifungal activities of ligand and complexes are shown in table 6. The inhibition of fungal growths expressed in terms of percentage was determined on the growth in test plates compared to the respective control plates as a percent of inhibition. *A. niger* was more sensitive (35.1%) against all the tested compounds compared with other filamentous fungi. The Ni(II) complex is most effective against *A. niger* and *P. expansum*. On the other hand, *A. flavus* and *A. alternata* were more sensitive to Fe(II) complex. The Ni(II) and Fe(II) complexes are more effective against filamentous fungi than the free ligand. Previous studies have shown that the Ni(II) and Fe(II) complexes have antimicrobial activity [17, 45, 46] and metal chelates have higher antimicrobial activity than the free ligand [45, 47]. Such an increased activity of the complex can be explained on the basis of overtone's concept and chelation theory [48]. The complex may disturb the respiration process of the cell and thus block the synthesis of proteins [49].

4. Conclusion

Tridentate Schiff base **HL1** and its Ni(II) and Fe(II) complexes were synthesized and characterized. The single crystal X-ray structures of **1** and **2** show a distorted octahedral geometry around Ni(II) and Fe(II). **HL1** is a monobasic neutral tridentate ligand coordinating through alkoxy oxygen, imine nitrogen, and phenolic oxygen via deprotonation. The free ligand and complexes were screened for the antibacterial and antifungal activities by

disk diffusion, microdilution broth, and single spore culture techniques. The antimicrobial activities show that the free ligand and its metal complexes exhibit antimicrobial properties. In comparison to the ligand, the metal complexes were more biologically active.

Supplementary material

Crystallographic data for the structure reported in this paper have been deposited with the Cambridge Crystallographic Data Center (The Director, CCDC, 12 Union Road, Cambridge, CB2 1EZ, UK; E-mail: deposit@ccdc.cam.ac.uk; www: <http://www.ccdc.cam.ac.uk>; Fax: +44 1223 336033) and are available free of charge on request, quoting Deposition Nos. CCDC 8866731 and 866732.

Acknowledgments

The financial support from the Scientific and Technical Research Council of Turkey (TUBITAK) Grant No: TBAG-108T431 and the Research Funds of Balikesir University (BAP-2010/122) is gratefully acknowledged. Dr Kara also thanks the Nato-B1-TUBITAK for funding and Prof. Guy Orpen (School of Chemistry, University of Bristol, UK) for his hospitality.

References

- [1] B.J. Gangani, P.H. Parsania. *Spectrosc. Lett.*, **40**, 97 (2007).
- [2] M.S. Masoud, A.E. Ali, M.A. Shaker, G.S. Elasala. *Spectrochim. Acta, Part A*, **90**, 93 (2012).
- [3] V.K. Chityala, K. Sathish Kumar, N.J.P. Subhashini, P. Raghavaiah. Shivraj, *J. Coord. Chem.*, **66**, 274 (2013).
- [4] C. Anitha, C.D. Sheela, P. Tharmaraj, S. Johnson Raja. *Spectrochim. Acta, Part A*, **98**, 35 (2012).
- [5] G. Budige, M.R. Puchakayala, S.R. Kongara, A. Hu, R. Vadde. *Chem. Pharm. Bull.*, **59**, 166 (2011).
- [6] G. Kumar, A. Kumar, N. Skishodia, Y.P. Garg, B.P. Yadav. *E. J. Chem.*, **8**, 1872 (2011).
- [7] D. Arish, M. Sivasankaran Nair. *Spectrochim. Acta, Part A*, **82**, 191 (2011).
- [8] B. Geeta, K. Shrivankumar, P. Muralidhar Reddy, E. Ravikrishna, M. Sarangapani, K. Krishna Reddy, V. Ravinder. *Spectrochim. Acta, Part A*, **77**, 911 (2010).
- [9] G. Kumar, S. Devi, R. Johari, D. Kumar. *Eur. J. Med. Chem.*, **52**, 269 (2012).
- [10] O.M.I. Adly. *Spectrochim. Acta, Part A*, **95**, 483 (2012).
- [11] M.B. Halli, R.B. Sumathi. *J. Mol. Struct.*, **1022**, 130 (2012).
- [12] G. Kumar, D. Kumar, S. Devi, R. Johari, C.P. Singh. *Eur. J. Med. Chem.*, **45**, 3056 (2010).
- [13] Z.A. Siddiqi, M. Khalid, S. Kumar, M. Shahid, S. Noor. *Eur. J. Med. Chem.*, **45**, 264 (2010).
- [14] H. Chen, J. Rhodes. *J. Mol. Med.*, **74**, 497 (1996).
- [15] H.J. Smith, C. Simons. *Proteinase and Peptidase Inhibition: Recent Potential Targets for Drug Development*, Taylor and Francis, London (2001).
- [16] R.R. Zaky, K.M. Ibrahim, I.M. Gabr. *Spectrochim. Acta, Part A*, **81**, 28 (2011).
- [17] X. Zhu, C. Wang, Z. Lu, Y. Dang. *Transition Met. Chem.*, **22**, 9 (1997).
- [18] V.P. Daniel, B. Murukan, B. Sindhu Kumari, K. Mohanan. *Spectrochim. Acta, Part A*, **70**, 403 (2008).
- [19] Z. Xinde, L. Zhifeng, W. Zhishen. *J. Inorg. Chem. (Russ.)*, **36**, 1748 (1991).
- [20] K.R. Surati. *Spectrochim. Acta, Part A*, **79**, 272 (2011).
- [21] H.F. Abd El-halim, M.M. Omar, G.G. Mohamed. *Spectrochim. Acta, Part A*, **78**, 36 (2011).
- [22] E. Gungor, S. Celen, D. Azaz, H. Kara. *Spectrochim. Acta, Part A*, **94**, 216 (2012).
- [23] K.A. Weber, L.A. Achenbach, J.D. Coates. *Nat. Rev. Microbiol.*, **4**, 752 (2006).
- [24] K.L. Straub, M. Benz, B. Schink. *FEMS Microbiol. Ecol.*, **34**, 181 (2001).
- [25] Bruker – AXS SAINT V7.60A.
- [26] G.M. Sheldrick, *SADABS V2008/1*, University of Göttingen, Germany (2008).
- [27] G.M. Sheldrick, *SHELXTL Version 5.1, Program for the Solution and Refinement of Crystal Structures*, Bruker AXS, Inc., Madison, WI, USA (1999).
- [28] H.D. Flack. *Acta Crystallogr.*, **A39**, 876 (1983).
- [29] A.L. Spek. *J. Appl. Crystallogr.*, **36**, 7 (2003).

- [30] National Committee for Clinical Laboratory Standards, *Performance Standards for Antimicrobial Disc Susceptibility Test*, 6th Edn., Approved Standard, M2-A6, NCCLS, Wayne, PA (1997).
- [31] E.W. Koneman, S.D. Allen, W.M. Janda, P.C. Srecekberger W.C. Winn, *Colour Atlas and Textbook of Diagnostic Microbiology*, p. 785, Lippincott–raven Publishers, Philadelphia, PA (1997).
- [32] I. Hasenekoglu, *Laboratory Techniques for Microfungi*, p. 66, Ataturk University, Erzurum, Turkey (1990).
- [33] F. Hadecek, H. Greger. *Phytochem. Anal.*, **11**, 137 (2000).
- [34] N. Dharmaraj, P. Viswanathamurthi, K. Natarajan. *Transition Met. Chem.*, **26**, 105 (2001).
- [35] M. Dey, C.P. Rao, P.K. Saarenketo, K. Rissanen. *Inorg. Chem. Commun.*, **5**, 924 (2002).
- [36] Y.M. Chumakov, V.N. Biyushkin, T.I. Malinovskii, V.I. Tsapkov, M.S. Popov, N.M. Samus. *Koord. Khim.*, **17**, 1398 (1991).
- [37] J. Han, Y.H. Xing, F.Y. Bai, X.J. Zhang, X.Q. Zeng, M.F. Gez. *J. Coord. Chem.*, **62**, 2719 (2009).
- [38] M.D. Godbole, M.P. Puig, S. Tanase, H. Kooijman, A.L. Spek, E. Bouwman. *Inorg. Chim. Acta*, **360**, 1954 (2007).
- [39] S. Banerjee, J.T. Chen, C.Z. Lu. *Polyhedron*, **26**, 686 (2007).
- [40] A.A.A. Emara, O.M.I. Adly. *Transition Met. Chem.*, **32**, 889 (2007).
- [41] A.A.A. Emara, B.A. El-Sayed, E.A.E. Ahmed. *Spectrochim. Acta, Part A*, **69**, 757 (2008).
- [42] D. Baudoux, Antiviral and antimicrobial properties of essential oils. Available online at: www.aromabar.com/articles/aud55.htm (accessed 18 April 2013).
- [43] Z.H. Chohan, H. Pervez, A. Rauf, A. Scozzafava, C.T. Supuran. *J. Enzyme Inhib. Med. Chem.*, **17**, 117 (2002).
- [44] S.K. Sengupta, O.P. Pandey, B.K. Srivastava, V.K. Sharma. *Transition Met. Chem.*, **23**, 349 (1998).
- [45] M. El-Behery, H. El-Twigry. *Spectrochim. Acta, Part A*, **66**, 28 (2007).
- [46] K. Singh, M.S. Barwa, P. Tyagi. *Eur. J. Med. Chem.*, **41**, 147 (2006).
- [47] R. Nair, A. Shah, S. Baluja, S. Chanda. *J. Serb. Chem. Soc.*, **71**, 733 (2006).
- [48] N. Raman, V. Muthuraj, S. Ravichandran, A. Kulandaisamy. *Proc. Indian Acad. Sci.*, **115**, 161 (2003).
- [49] N. Raman, A. Kulandaisamy, C. Thangaraja, P. Manisankar, S. Viswanathan, C. Vedhi. *Transition Met. Chem.*, **29**, 129 (2004).